2017

Band Gap Engineering Of Titania Systems Purposed For Photocatalytic Activity

Cameron Robert Thurston
University of Mississippi

BAND GAP ENGINEERING OF TITANIA SYSTEMS

PURPOSED FOR PHOTOCATALYTIC ACTIVITY

A Thesis
presented in partial fulfillment of requirements
for the degree of Master of Science
in the Department of Mechanical Engineering
The University of Mississippi

by

CAMERON THURSTON

May 2017

ABSTRACT

Ab initio computer aided design drastically increases candidate population for highly specified material discovery and selection. These simulations, carried out through a first-principles computational approach, accurately extrapolate material properties and behavior. Titanium Dioxide (TiO_2) is one such material that stands to gain a great deal from the use of these simulations. In its anatase form, titania (TiO_2) has been found to exhibit a band gap nearing 3.2 eV. If titania is to become a viable alternative to other contemporary photoactive materials exhibiting band gaps better suited for the solar spectrum, then the band gap must be subsequently reduced. To lower the energy needed for electronic excitation, both transition metals and non-metals have been extensively researched and are currently viable candidates for the continued reduction of titania's band gap. The introduction of multicomponent atomic doping introduces new energy bands which tend to both reduce the band gap and recombination loss. Ta-N, Nb-N, V-N, Cr-N, Mo-N, and W-N substitutions were studied in titania and subsequent energy and band gap calculations show a favorable band gap reduction in the case of passivated systems.

LIST OF ABBREVIATIONS

DFT	Density Functional Theory
DSSC	Dye Sensitized Solar Cell
QDSC	Quantum Dot Solar Cell
TTIP	Titanium Isopropoxide
CVD	Chemical Vapor Deposition
LFT	Ligand Field Theory
TM	Transition Metal
CBM	Conduction Band Minimum
VBM	Valence Band Maximum
GGA	Generalized Gradient Approximation
LDA	Local-density Approximation

ACKNOWLEDGEMENTS

I would like to take this chance to thank my advisor, Dr. Amrita Mishra and Dr. Gautam Priyadarshan for the tremendous opportunity to take part in this fascinating aspect of materials science research. Their focus and guidance ensured that my experience here at The University of Mississippi helped to develop skills I will carry with me indefinitely. I would also like to sincerely thank Dr. Pandya and Dr. Rajendran for serving on my defense committee. I would also like to thank Matt Nelms, whose guidance and perspective I consider to be invaluable as I continue onward.

Also, I would thank Dr. Jim Chambers whose contagious passion and humor within academia was felt by all those who had the privilege to know him. His genuine passion for both formal education and life-long learning was the deciding factor in my attendance of Graduate School here at Ole' Miss. His inclusive spirit made the transition from my undergraduate to graduate academic career extremely easy. He will be profoundly missed and remembered.

Finally, I would like to thank Will Earwood. Throughout my graduate career Will made himself available to lend a hand and provide invaluable support. His necessary input and direction helped to fundamentally shape my work.

Calculations reported in this work were carried out on equipment funded by the U.S. Army Research Office under a cooperative agreement award contract No. W911NF-11-2-0043

and the U.S. Army Engineering Research and Development Center's Military Engineering Basic/Applied "MMFP" Research Program.

TABLE OF CONTENTS

TABLE OF FIGURES

TABLE OF TABLES

CHAPTER 1

INTRODUCTION

1.1 Introduction

The introduction of titanium dioxide as a photocatalytic material began in 1972 when the Honda-Fujishima team showed that under solar irradiation TiO_2 induced photolysis of water [1]. Since that time, there has been a dramatic increase in research into the various capacities of titanium dioxide as a functional material. Titanium dioxide today is used in biomedicine [2], paint [3], photolysis [1] [4], sunscreen [5], dye sensitized solar cells [6], and gas sensing technologies [7] [8]. TiO_2 both alone and in conjunction with other materials stands to dramatically improve energy, environmental, and safety issues facing the consumers today.

The appeal of titanium dioxide (titania) as it pertains to immediate research value is the cost and tenability of the metal in the world marketplace. Titanium products are advantageous in that cost is relatively cheap, they're easily obtainable, chemically stable, and thoroughly market tested. As an added benefit, titania is a robust metal oxide with total non-toxicity to consumers. As a result, research into the improvement and fundamental understanding of this material is inherently worthwhile in any respect.

Of the many uses of titania, its potential as a photovoltaic material is extremely compelling. Its benefits are compounding in fields such as energy and environmental engineering as they face challenges which require immediate yet effective solutions at low costs. In this respect, titania stands to replace currently used systems which require costly manufacturing and

materials costs. If titania is to become a viable candidate for replacement of traditional solar cell technology, there first must be a drastic improvement of its electrical activity under the solar spectrum. As it currently stands, titania is most electrically active under ultraviolet light.

Titania has 3 distinct polymorphs which exist within nature. The first mineral phase, rutile, has a band gap of 3.0 eV which is the lowest of the three. Anatase and brookite both have higher band gap values of 3.2 eV and 3.4 eV respectively. Of the three, anatase is considered to be the prominent candidate for photocatalytic activity [9]. The reason for this discrepancy between increased photocatalytic activity and higher band gap is not yet universally agreed upon by scientists.

1.2 Anatase vs Rutile Electrical Properties

There are multiple explanations as to why the photocatalytic activity is higher for anatase titania. The earliest contentions hold that charge transport considerably differs between the 3 polymorphs. Materials similar in nature to TiO_2 have been previously found to exhibit anisotropic electron excitation along different crystallographic planes [10]. This anisotropic reactivity was an initial explanation as to why rutile performed poorly in solar cells utilizing photosensitizing dyes in initial investigations. Reactivity notwithstanding, electron diffusion along different planes is a significant factor explaining the photocatalytic difference between mineral crystal structures. Reported packing densities of 3.8-3.9 g/cm^3 for anatase and 4.2-4.3 g/cm^3 for rutile also help to explain electron mobility differences [11]. Large differences in electron diffusion and reactivity together illuminate as to why rutile performs poorly when compared to anatase.

Researchers also contend that electron-hole recombination is more prevalent in materials exhibiting a direct band gap as opposed to an indirect band gap. Indirect band gaps are

characterized by the maximum of the valence band and the minimum of the conduction band being dissimilar in k-vectors. This dissimilarity in k-vectors alludes to 'misaligned' bands which requires phonon assistance for excited electron to be absorbed into the conduction band. However, for those materials with direct band gaps, the crystal momentum need not change and no phonon assistance is required. It is believed that it is these momenta changes which discourage subsequent electron-hole recombination in materials exhibiting indirect band gaps. Figure 1 demonstrates the recombination process by which an electron is reabsorbed into the valence band. Preliminary investigations have theoretically indicated that the rutile phase

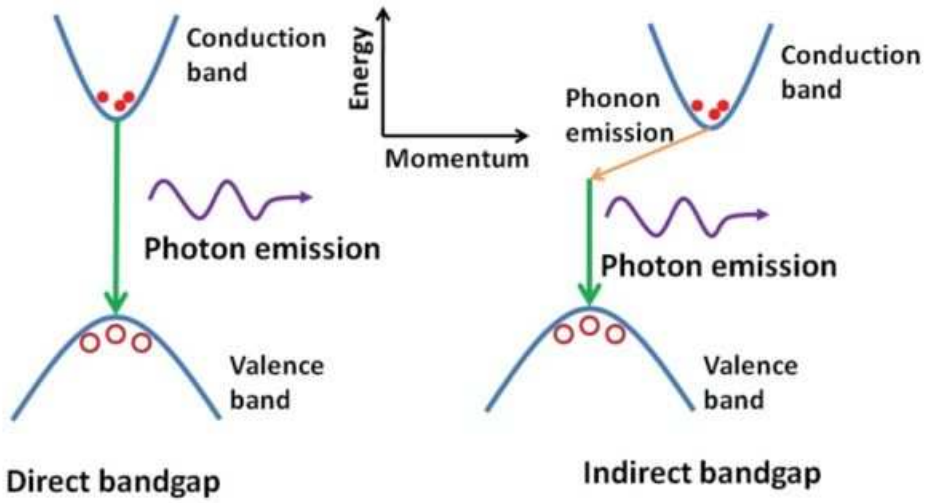

Figure 1: Direct and indirect band gaps [71]

contains preferential direct band gap differences [12]. The characteristic direct band gap of rutile and the theorized longer exciton lifetime of indirect band gaps explains the better photocatalytic activity of anatase [13].

For systems working in conjunction with titania, there is a predicted oxidative effect for materials exhibiting higher valence bands. Titania is thought to have photocatalytic activity via its higher valence band relative to the redox potential of an absorbed molecule. This higher

valence band implies an increased oxidative power of those electrons ejected from the valence band and an overall increase in electron transfer to the absorptive matrix [9].

1.3 Surface Morphology

Surface properties are also a mitigating factor at play with the reduction in photocatalytic capacity of rutile titania. Investigations into surface effects outlining differences in polymorph performance proved themselves extremely valuable. Wilson J. et al. found that different surface morphologies and orientations could be playing an important role in reactivity [14]. It was found that the {011} faceted surface was much more reactive than the compared {014} surface. Luttrell et al. reviewed studies and outlined the effect of defects and well-ordered surface morphologies on molecule absorptive differences, electronic structure (charge trapping), potential differences with interacting surfaces, and electrochemical reactivity [9]. These surface effects and the different surface morphologies existent between anatase and rutile structures help to explain increased electronic performance in the anatase polymorph.

The determination of photosensitivity and conduction via surface structure was a considerable factor in the rise of titania as a candidate material in electronic property studies. And with the growth of nanomaterial study and use, titania gained another avenue through which it could be employed. Nanomaterials, as defined by the European Commission, are "particles, in an unbound state or as an aggregate or as an agglomerate and where, for 50% or more of the particles in the number size distribution, one or more external dimensions is in the size range 1 nm – 100 nm" [15]. And with relation to titania specifically, the majority of its uses stem from its ability to be synthesized with extremely small particle dimensions. The properties derived from unique nanostructures allow for significantly superior performance in a variety of contemporary uses. In 2004, it was found that TiO_2 nanotube array gas sensors at room temperature exhibit a

1,000,000,000% change in electrical resistance compared to similarly designed sensors [16]. The drastic electrical enhancement in gas sensing ability was reported to be a direct result of the structural morphology of the titania generated.

1.4 Doped titania nanomaterials synthetic methods

Unlike traditional photocatalytic materials, titania nanomaterials can be synthesized rapidly [7]. When considering photocatalysis, increasing the active area of exposure lends itself to be essential for consideration in materials processing moving forward. Change in active exposure area changes the total flux, photon power density, which consequently increases photolysis. Nano-rods, fibers, tubes, clusters, and similar structures are all employed to increase the active surface area of a substance. Nanotube growth has been theoretically predicted to improve the structural and electrochemical behavior of titania's photocatalytic effects [17].

The introduction of nanoscale surface purposing therefore has the capacity to drastically improve the photosensitivity of titania. Surface purposing is carried out through the introduction of structures and electrochemical bonds specifically tailored to produce maximal photocatalytic behavior. Bulk chemical doping through the introduction of foreign elemental constituents is yet another means through which red shifting of band gaps is achieved. Doped titania nanomaterials working in conjunction with nanoscale purposing is fabricated through a variety of methods. For doped titania systems, current popular methods include:

1. Wet Chemistry Synthesis
2. Mechanical & High Temperature Treatments
3. Ion Implantation

Synthesis of doped titania nanomaterials via wet chemistry is accomplished through a variety of means. A widespread selection among these is the sol-gel method; where a titanium

precursor is hydrolyzed into a colloidal solution with subsequent precipitation of the oxide through heating or redox reactions. This method allows for controlled particle size and ion dopant concentration. For titania nanomaterials, titanium(IV) alkoxide and titanium isopropoxide (TTIP) are commonly used with metal ion doping in their synthesis. Such doping in sol-gel systems has been experimentally shown to significantly affect the characteristic photocatalytic activity [18].

High temperature treatments synthesizing doped titania nanomaterials are extremely popular and comprise the vast majority of experimental synthesis. Among these, the solution combustion method persists as it rapidly generates highly controlled doped titanium oxides. Unlike sol-gel, ion implantation, and liquid phase deposition methods, solution combustion doesn't require reagents or post-treatment time therefore reducing both cost and total generation time. A fuel like glycerin or urea is hydrolyzed with the addition of a precursor. In the case of titanium dioxide, these precursors often include titanyl nitrate with the inclusion of a controlled dopant nitrate [19]. The resulting solution is then dehydrated and combusted which results in the final nanomaterial synthesis.

Ion-implantation is another means through which doped nanoparticles are synthesized. In this method, an ionizing chamber releases ions which are accelerated through a magnetic field to speeds capable of depositing them into the subject material. The depth and breadth of beam penetration is controlled so as to control dosing of ions. However, the exact crystal composition and structure is difficult to control. The structural damage associated with ion doping historically limited it in its use for photocatalytic use. It was found that through that the introduction of thermal annealing the amorphous structure of titania as a result of ion-implantation can be reversed back to its anatase crystallinity [20].

Chemical vapor deposition (CVD) remains a popular alternative method for the generation of thin films of doped nanomaterials. In this process a gaseous chemical precursor is electrochemically deposited onto a substrate, often glass, at thicknesses capable of being below 10nm. In the case of titania, titanium isopropoxide is often the subject of pyrolysis in an oxygen/helium environment. The heated gas then deposits amorphous TiO_2 onto the reactor at temperatures below 90□ [7]. Mills et al. reports that a photoactive TiO_2 nanofilm was successfully achieved through CVD at ambient pressures [21]. Titania's success in the CVD technique at atmospheric pressures further demonstrates its suitability for large scale production. Studies like those from Mills et al. provide insight onto the various means of development available to titania as it progresses as a nanomaterial and photosensitive material.

1.5 Conclusion

With 81% of U.S. energy generation sourced from fossil fuel technology [22] , it becomes infeasible to focus on continued development into a fuel source with known short term limitations. Considerations for greenhouse gas emissions further demonstrate the changing need for diversified energy sourcing.

As such, much of the industry focus has been directed towards silicon based photovoltaics thereby leaving much of the other viable technologies lagging. Figure 2 shown below outlines photovoltaic conversion efficiencies for current photo-conversion methods. It's evident that those technologies lowest in efficiency are those technologies existing outside of Silicon and Gallium Arsenide. Long term solutions to meet energy demands of a growing market necessitate diversified sources for solar power. To meet future power demands and engineering specifications, titania and materials like it provide a means for alternative solar power production.

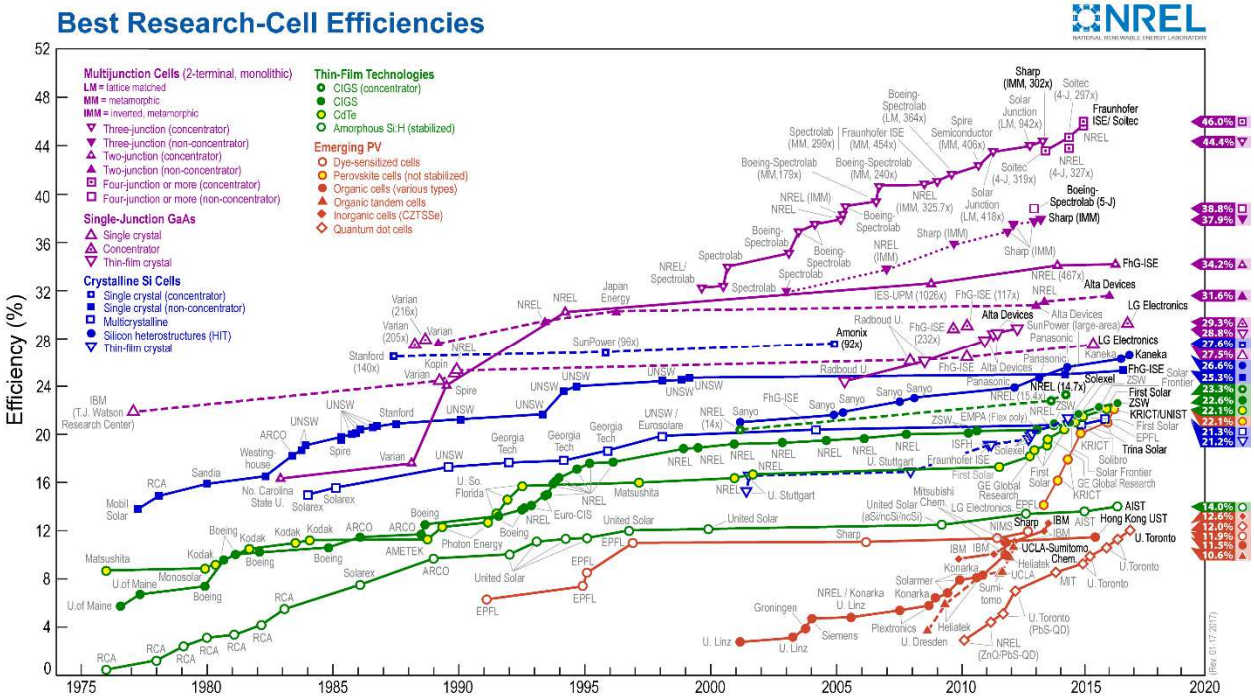

Figure 2: Cell efficiency development over time [69]

CHAPTER 2

BACKGROUND

2.1 Grätzel Cell

In 1991 the concept for a low cost photovoltaic cell was developed and titania was thrust into the forefront of novel photovoltaic materials [6]. This technology, known as the Dye sensitized solar cell (DSSC), was developed by Michael Grätzel and Brian O'Reagan with an energy conversion efficiency near 7%. For his pioneering work in the field of energy and electron transfer, Grätzel received numerous technological prizes and commendations including the 2010 Millennium Technology prize.

The design of DSSC construction relies on principles analogous of traditional silicon based structures. Instead of photo-conversion utilizing a traditional p-n junction where both p and n-type semiconductors are of similar base material, DSSC design relies on the integration of a photosensitizing dye into a mesoporous titania substrate. This photosensitive dye, capable of being either organic or inorganic, injects an excited electron into the anodic titania surface. The electron is then conducted away thereby generating a circuit current. At the same time, the photosensitive dye is returned to its ground state via a redox reaction with a mediator and subsequently the mediator with the cathode. This process of excitation, reduction and oxidation of the photosensitive dye is carried out billions of times per second to generate a current [23].

Figure 3 outlines the principle electrochemical mechanisms allowing for DSSC operation. At this juncture, the peak for laboratory grade DSSC efficiency stands at 15%.

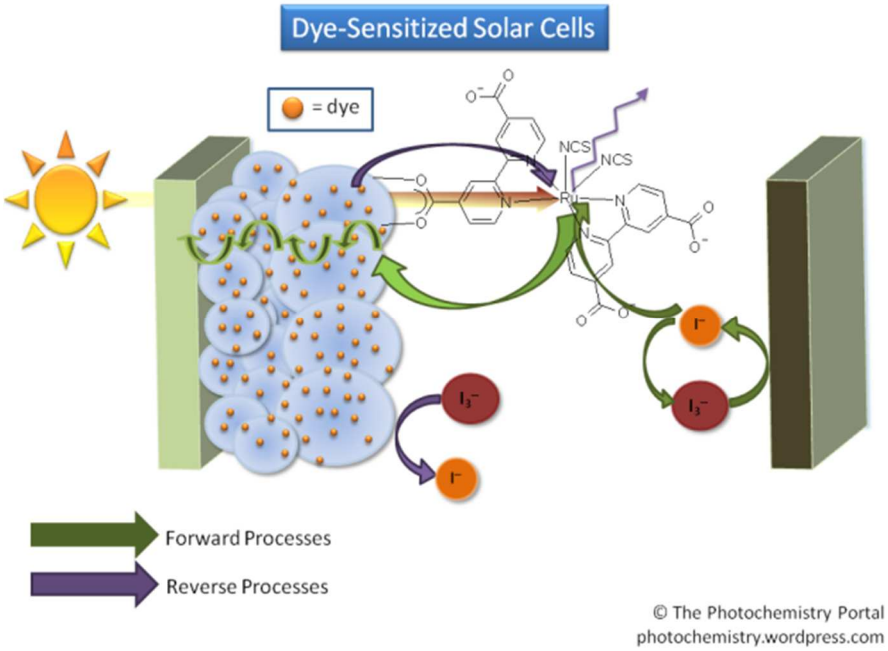

Figure 3: DSSC operation principles [70]

The advantage of using titanium dioxide systems within DSSC systems stems from its long lifespan before eventual decomposition and mechanical failure. The robust mechanical and electrochemical structure of titania with respect to its inexpensive cost reduces waste and increases viability for competition in energy markets.

Challenges facing dye sensitized nanostructured materials today relate specifically to the wide band gap and thermal sensitivity of titania's electro-structure. To reduce thermal degradation, electron-hole pair recombination, and fermi levels to suitable values it becomes obvious that a photocatalytic purposing of titania is needed. Doping is the means through which this purposing of metallic materials is often achieved. This process introduces impurities into the lattice thereby deforming the structure, modifying orbital hybridization, and introducing

additional available electrons for conduction. Crystal deformations and orbital hybridization are predicted to be provide significant impact on the bulk electronic response in semiconducting materials. Characteristic bond forces and their angles are additionally well known to be directly responsible for thermal nature bulk materials.

2.2 Quantum Dot Solar Cell

As it stands today, titania could potentially exhibit a band gap well within the range needed for traditional photovoltaic technology existent today. Modern photovoltaic material operates on the principle of the two biased semiconducting materials and their interaction with one another. After a photon with sufficient energy has created an exciton from the valence band of the p-type semiconductor the electron is conducted via an intrinsic junction potential to the n-type semiconductor.

Recently, there has been a rapid development into the improvement of mesoscale semiconducting materials further broadening the scope of photo-catalytically purposed titania. Known as Quantum Dot Solar Cells (QDSC), this technology provides the ability to tune mesoscopic materials' band gaps into the visible region. This is accomplished through the introduction of quantum dots. Through a change in their respective size, these dots are able to adjust their band gaps. Through the introduction of an additionally photo-catalytically tuned Titania bulk material, QDSC technology has been shown to improve a great deal [24] [25]. Ultimately, this improvement is still severely lacking when considering the pronounced changes needed in structure for market viability.

2.2 Band Gap Tuning

To gain substantial viability for consumer energy production, it became necessary to tune band gaps to better suit photo activity and current generation. Dürr et al. used mixed Ti-Zr oxides

to tune conduction and valence bands to better suit a DSSC system. It was found that for small values of Zirconium doping increased the open circuit potential and increased overall power generation [26]. This increase in power generation was attributed to the mixed oxide system having a blue-shifted conduction band allowing for absorption of high energy electrons. Additionally, the blue shift in the conduction band is thought to decrease recombination rates via increased band differences. However, higher values of zirconium doping prevented electron absorption and decreased overall power conversion. Dürr concluded that dye excitation tuning and semiconductor optimization are necessary for complete use of the solar spectrum.

Kılıç et al. introduced Fe_2O_3 as an oxide dopant in nanostructures to improve photocatalytic conversion in DSSC electrodes. Introducing both nanostructures and dopant mixing were thought to increase the efficiency in electrical conversion. Kılıç et al. reports that these nanostructures in conjunction with Fe_2O_3 increased solar conversion to 7.27% from 5.25% from pure anatase [27]. It becomes obvious that nanoscale studies with mixed oxide concentrations are necessary for improving the performance of DSSC. Such studies stand to improve performance; however, they are limited by the scale at which these cells perform. These studies, though essential for candidate validation, are extremely time consuming and intensive for candidate viability.

Titania doping explorations are often characterized by the dopant material class, as particular classes tend to exhibit unique properties. Metal-ion doping remains extremely popular and numerous studies showed early on that their introduction causes significant band gap shift into the visible spectrum [28]. However, recombination losses and minimal band structure change have been persistent issues facing many of the transition metal doped systems purposed for photo-activity. Consequently, another dopant candidate class grew which consisted of non-

metals [29] [30] [31]. These dopants prove themselves to be promising candidates for both increasing photo-activity in the visible spectrum and reducing recombination losses. Even more crucial is that their insertion into the crystal lattice does not cause a shift into an amorphous structure like many of the metal-ion dopants.

Quantum level studies aim to understand governing relationships and predict results from such studies. The introduction of quantum scale calculations with software packages like CASTEP allows insight into the fundamental concepts governing photocatalytic performance in materials. By altering the stoichiometry and associated wave functions governing a given crystal, scientists are able to theoretically derive these band gap results without ever having generated a physical material.

2.3 Ab Initio Modeling

Ab initio studies use what is known as a first principles approach to sort through candidates and develop sophisticated predictions as to ideal atomic compositions. This approach relies on knowledge of known quantum mechanical interactions to yield an overall prediction for a particular crystal system's properties. Atomic interactions govern the entirety of the material properties; therefore, calculating the probabilistic result of a given system's wave function reliably describes its physical characteristics. Every quantum mechanical calculation aims to appropriately account for electron interactive forces, electron-nucleus and intra-nucleus attraction. As it stands, the fundamental equations surrounding these energetic relationships are intractable. To that effect, it is extremely computationally expensive to simply estimate these interactions to a high degree of accuracy using traditional Schrödinger equation established methods. Approximations are made to lessen this computational load through the use of a variety of functionals which describe the electronic nature of the given solid [32]. By describing the

series of interactive forces governing a system as a series of functionals which are formulated by DFT, scientists are able to computationally sidestep solving the Schrödinger equation and its many-body wave problem.

There exist numerous computational approaches created to predict user created crystal systems. One such method, CASTEP, employs the use of Density Functional Theory (DFT) to evaluate properties of a user defined crystal structure. It is now possible through the use of modules like CASTAP to characterize optical and electronic behavior of a theoretically defined crystal. Early ab initio studies into titanium dioxide immediately concerned themselves with the electronic properties and structure of the compound as decades of promising research had shown its capacity as a photocatalyst [33] [34] [35]. Early DFT research into crystal structure [36] and chemisorption [37] provided insight onto titania's intrinsic value as a potential photovoltaic material.

As its popularity grew, studies began to emerge concerning themselves with theoretically altering the band gap of the material through the introduction of crystal defects. Vacancy, interstitial, and substitutional defects are commonly studied in theoretical titania crystals in hopes of generating a material with an ideal band gap. Common early defects consisted of metal ion dopants which were found to effectively tune the band gap to a range bridging the visible spectrum [38] [39]. As candidate population and studies concerning them increased, it became worthwhile to use ab initio studies as a means to direct future experimental candidate studies. Asahi et al. was the earliest report from a research group introducing computer aided design in this directive capacity [40]. It is this novel aspect of research which began an influx of studies concerning themselves with theoretical band gap modification and characterization. Asahi et al.

shifted much of the research focus entirely from metal ion substitution to substitutions and interstitial doping comprised of nitrogen.

Asahi et al. contends that the narrowed band gap of the nitrogen doped titania system was the result of band hybridization of O 2P states with N 2P states resulting in a raised valence band energy state. This contention holds today although there exist alternative explanations as to why non-metal doping remains the effective method of band gap modification. One explanation holds that the introduction of nitrogen introduces a narrow band slightly above the valence band of TiO_2 [41]. This proposed band suggests that the characteristic energy levels associated with TiO_2 are not changed through nitrogen substitution. Rather, nitrogen itself introduces its own localized band into the material band structure. The alternative proposition holds that an oxygen deficiency from nitrogen presence within the crystal results in a lowered CB state of the remaining oxygen [42] [43].

Today it remains unclear as to which explanation is definitively true. However, it remains that the introduction of a dopant species into the crystal structure has tremendous power in shaping the electronic behavior of titania. Further discussion of the effects of theoretical doping can be found in Chapter 3.

2.4 Conclusion

The increase in solar cell technologies and methodology spurred an examination into the various materials capable of photocatalysis. Titania, through decades of peer-reviewed research, proves itself to be an extremely viable photoactive material. It endures as a material incredibly robust in processing yet is economical for large scale fabrication. These qualities, as well as its non-toxicity, compound to identify titania as worthy of continued study. Its experimental proof

of concept from the development of the Grätzel Cell further realized its capacity as a photosensitive material.

An effective alternative material suited for photovoltaics like titania provides the diversification necessary for a sustainable long term solution to world energy needs. Band gap tuning follows naturally to purpose titania to meet specialized conversion needs. The introduction of dopants introduces intermediary energy states which further reduces the band gap and shifts the fermi energy.

Ab initio studies provide a platform for significant population growth. Through effective modeling, fundamental aspects governing a crystal system are better understood and explained. It follows naturally that through modules like CASTEP candidate preselection circumvents a large majority of superfluous study. Ab initio study into a material such as titania stands to drastically reduce production time.

CHAPTER 3

CONCEPTUAL BACKGROUND

3.1 Group Theory

Central to the ideas surrounding band structure engineering and modeling are the fundamental aspects comprising crystal structures and lattices. Electronic behavior of materials is an important aspect followed from their principal crystal symmetry. Building a complete model within CASTEP requires an associated space group to define the particular geometric and crystal characteristics. There exist 230 space groups comprised from 32 point groups and 14 Bravais lattices. Crystal generation is initiated through a basis combination into the lattice via a process known as convolution. Convolution is the method through which a copy of a basis is made in agreement with a series of mathematical operations. The operations constraining this new basis location can result in inversion, rotation, and reflection. The 32 crystallographic point groups result from the various configurations generated from these operations. After an individual unit cell is represented, an infinite array is generated through a set of translation vectors to achieve a unique crystalline arrangement. These infinite arrays, named Bravais Lattices, exist in 14 uniquely defined arrays. Anatase titania exists in a tetragonal $I4_1/amd$ spacegroup with lattice parameters $a=b\neq c$.

3.2 Band theory

Critical to understanding band gap modification remains the band theory which describes electron behavior of a solid state system. Electrons as fermions, due to the Pauli-Exclusion principle, can only exist in one of two states in an orbital. As the population of constituent atoms is increased, the atomic energies vary slightly to obey the Pauli-Exclusion principle. The result of these interacting orbitals, known as molecular orbitals, represent the split energy levels of all atomic orbitals populated within a crystal [44]. As the constituent molecular orbitals are increased to large values ($N > 10^{22}$) the molecular orbitals begin to form a continuum known as a band. The electron concentration in band theory in a material is found through the use of the Fermi-Dirac distribution $f(E)$ defined:

1

$$f(E) = \frac{1}{1 + e^{\frac{E-\mu}{k_b T}}}$$

For intrinsic semiconductors, the Fermi-Dirac distribution is combined through the density of states $g(E)$ to achieve a carrier concentration equation:

2

$$n = \int_{-\infty}^{\infty} g(E) f(E) dE$$

The application of band theory to the subject of crystal structures (esp. transition metals) forms a field of study known as Ligand Field Theory (LFT) whose scope extends beyond the focus of this thesis [45]. Ultimately, the result of these interactions as described by LFT make up the fundamental nature of known band structure relationships.

A semiconductor is a material whose valence and conduction bands, two distinct molecular orbital energy ranges, are separated by a what is commonly known as a forbidden band or band gap. This band gap, commonly represented as E_g, is formally characterized as the difference from CBM to VBM at a given point within the Brillouin zone. Within the study of

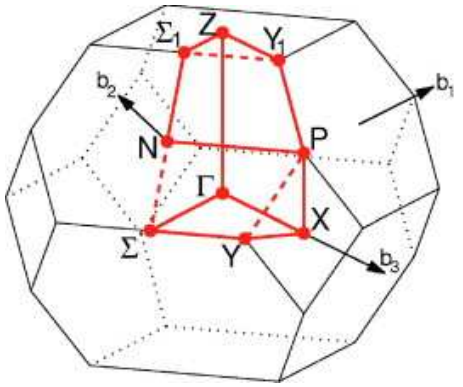

Figure 4: Body centered tetragonal Brillouin zone [73]

band structures, the center of the Brillouin zone (Γ) is of important consideration and is commonly the reference point for band gap study. This is a result of a number of factors. Reduced and periodic zone schemes are the two predominant plotting methods providing simplified representations of a demonstrated band gap. Both of these representations esthetically are centered on the center of the cell. Most importantly, it is also known that the first Brillouin zones centered at $k = 0$ (Γ) is representative of the primitive lattice cell [46]. Consequently, the Γ point is the center from which a band structure plot is constructed.

Characterizing semiconductors requires formal knowledge of what is known as the Fermi level. Born from Fermi-Dirac statistics, this level is formally known as the highest occupied electron energy level of a system's ground state. The significance born from this definition is that it indirectly describes the chemical potential for electrons in a given system. With the

introduction of doping, predicted shifts in the Fermi level describe the nature of the bond and the chemical potential shift born from its introduction into the lattice.

3.4 Doping

Doping with respect to traditional semiconductors has the capacity to increase electron or electron hole concentration within the crystal lattice. The introduction of substitutional or interstitial defects allows for the electronic structure of atomic impurities to permeate throughout the lattice. Atoms with similar electronic orbital structure containing auxiliary electrons injects these extra electrons into a band state thus biasing the material to become an electron donor. Those doping constituents providing less electrons for the crystal lattice are known as electron receptors. They provide receptor states which reverse bias electron mobility. These two dopant types, combined together with the intrinsic semiconducting material are known as n and p-type semiconductors, respectively. N and p-type semiconducting materials acting in conjunction are what serve as the basis for modern photovoltaic materials [47] [48].

In ab-initio studies, doping has been continually shown to have an effect in shaping large scale band structure changes [49] [50] [51] [52] [53]. Explaining energy state changes historically has been thought to be a result of orbital hybridization. In band theory, hybridization holds that the resultant energy of a hybrid orbital is approximated as the linear average of the contributing orbitals. It is therefore postulated that the orbitals generated from titania-TM d-orbital hybridization possibly contributes to a reduced CBM energy state. It follows that an additional oxygen-nitrogen 2p-orbital hybridization mentioned previously could also potentially contribute to a lowered VBM.

Aside from hybridization effects, there exist multiple alternate explanations concerning the introduction of non-metal doping with regard to structural energy changes. One of these

explanations involves doping introducing what are known as local states. These states are defined as quantum states which do not overlap significantly with those already established, essentially preventing the hybridization of orbital energies [54]. The resultant localized 2P energy states from nitrogen provides a theorized intermediary state above the previously un-doped valence band maximum thus reducing the overall band gap.

Vacancy defects also play a significant role in explaining the reduced band gap of TiO_2 upon nitrogen doping. It has been experimentally shown by groups like Di Valentin et al. that both nitrogen and carbon substitutional doping incurs a significant reduction in band gap [43] [55]. And subsequent DFT calculations have additionally shown the introduction of these species results in a lowered formation energy for oxygen vacancies. It naturally followed that these vacancy defects result in a lowered band gap. Vacancy band structure effects are a direct result of interacting wave functions of nearest neighbors. The removal of an oxygen atom within the titania crystal structure results in directly interacting orbitals of titanium. This indirect method of hybridization is thought to be another contributing factor behind non-metal doping in titania.

Titania co-doping, led by groups like Gai et al. and Long et al., drastically changed the method by which titania was engineered for a narrowed band gap [56]. Co-doping relies on the presence of multiple constituent dopants whose individual modifications to band structure complement to an overall dramatic increase in photocatalytic performance. In the case of titania, transition metal and non-metal co-doping remains the promising method by which co-doping is utilized in band tuning. The presence of both atomic elements increases the VBM and reduces the CBM as those elements achieved before in mono-doping. However, the orbital hybridization of the transition metal and non-metal dopant species is currently of particular interest. Multiple

studies contend that the presence of this hybrid orbital state mitigates possible isolated localized states and recombination loss.

3.5 Density Functional Theory

Computationally deriving the electronic behavior of solids becomes irresolvable with the use of traditional Hamiltonian methods derived from the wave functions of the Schrödinger equation. The many-body problem persistent when constructing a condensed-matter system prevents viable energy calculations to be performed on crystal systems. Density Functional Theory (DFT) radically changed the method by which the energy of a many-body system could be calculated at its ground state. DFT forgoes the wave function method through the introduction of functionals for electron density and the assumption that the variational minimum energy level is equal to the ground state energy [57]. Kohn and Sham showed it is indeed possible to replicate a many-body electronic system with a series of single-body electronic systems [58]. Instead of the Hamiltonian, total energy is expressed by way of:

3

$$E = E[\rho(\boldsymbol{r})] = \int d\boldsymbol{r} V_{ext}(\boldsymbol{r})\rho(\boldsymbol{r}) + F[\rho(\boldsymbol{r})]$$

Here the energy is expressed as the sum of the external potential energy present due to nuclei interaction and some energy functional dependent on the electron density $F[\rho(r)]$. This functional is defined as the sum of the Hartree Coulomb and electron kinetic energies with the addition of an exchange and correlation correction term.

4

$$F[\rho(\boldsymbol{r})] = E_K[\rho(\boldsymbol{r})] + E_H[\rho(\boldsymbol{r})] + E_{xc}[\rho(\boldsymbol{r})]$$

The Hartree Coulomb term is simply the potential energy present due to interacting electron clouds at radial spaces *r* and *r'* within the system:

5

$$E_H[\rho(\boldsymbol{r})] = \frac{e^2}{2}\iint \frac{\rho(\boldsymbol{r})\rho(\boldsymbol{r}')}{|\boldsymbol{r}-\boldsymbol{r}'|}d\boldsymbol{r}d\boldsymbol{r}'$$

The kinetic energy of the system is defined as:

6

$$E_K[\rho(\boldsymbol{r})] = \frac{\hbar^2}{2m}2\sum_i \int \psi_i{}^*(r)\nabla^2\psi_i(r)dr$$

Energy within DFT's formalism relies only on a radial variable in lieu of multiple positional coordinates representative of each electron's individual position relative to one another and the nucleus. The replacement of multiple positional vectors with a single radial vector drastically reduces the computational load necessary for calculations. Figure 5: Many-body versus DFT perspective, shown below, highlights the perspective of DFT in its aim to eliminate the multiple positional vector calculations.

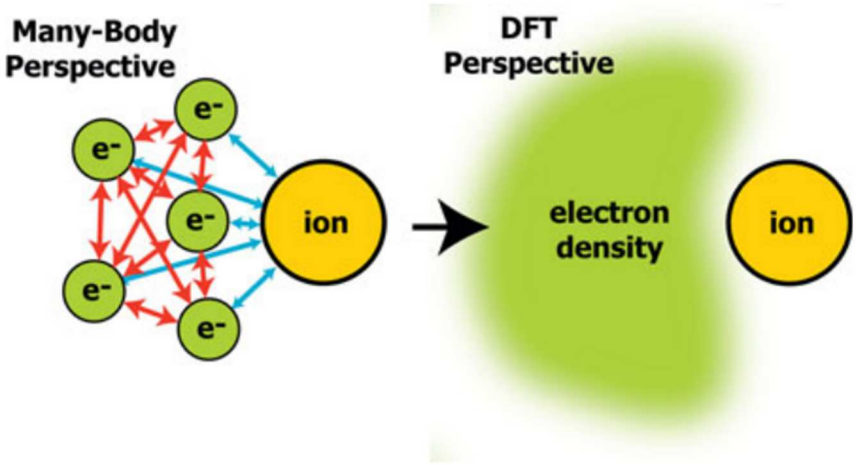

Figure 5: Many-body versus DFT perspective [59]

The density of a given system is given as the sum of the normalized wavefunctions of non-interacting electrons probed at some distance $\boldsymbol{r}$.

7

$$\rho(\boldsymbol{r}) = \sum_{n=1}^{N} |\psi_i(\boldsymbol{r})|^2$$

To resolve the reintroduction of wave functions into the formalism of DFT, Bloch's theorem is applied. Relying on plane wave methods, pseudopotentials and crystal periodicities, Bloch's theorem constructs wave functions for each electron in DFT as:

8

$$\psi_{n,k}(r) = \sum_{G} u_{n,k}(G) e^{i(k+G)*r}$$

Where $u_{n,k}$ is the periodic function representative of the periodicity of the crystal, *k* is the crystal plane wave number within the first Brillouin zone, and *r* is again the positional vector. The variable *G* included in the summation ensures such that the plane waves are in agreement with boundary conditions. This transition from traditional quantum mechanical descriptions of waves to Bloch's wave equation allows for tractable calculations of the electrons kinetic energy at certain points in crystal wave space [60].

Despite the Bloch's theorem providing an alternative route for the production of tractable wave functions, the plane-wave method is difficult to reproduce characteristic wave function nature. To resolve this difficulty a pseudopotential is applied to replicate the core electrons and their interaction with the electrons in the valence orbital. By doing so, calculations characterizing the associated orbital energy levels of atoms are feasible.

The remaining constituent, $E_{xc}[\rho(\boldsymbol{r})]$, is the corrective term which allows for accuracy in these calculations. Both the Hartree Coulomb and the kinetic energy term rely on the wave functions of non-interacting electrons. Obviously, electrons are always interacting with each other within a crystal system so a corrective term is therefore added to account for these

differences. Coulombic electron-core interactions changes when in the presence of additional electrons as does the overall kinetic energy. The exchange-correlation energy correction exists so as to more accurately describe the associated electron energies of these interacting systems. There exist a variety of mathematical approaches available to generate this corrective term, however LDA and GGA remain the two most widely used within academic research.

The sum total of these energies result in describing the overall energy of a given atomic system. This eloquent side step for solving of the Schrödinger equation allows for calculations of large electronic systems.

CHAPTER 4

METHODOLOGY

4.1 Relaxation Initialization

Doped anatase TiO_2 crystal systems with *I*41/*amd* space groups were extensively studied. Simulations were carried out to calculate electronic band structures and subsequent density of states. Relaxation simulations were first carried out to reflect equilibria values. The Perdew-Burke-Ernzerhof functional of the Generalized Gradient Approximation [61] (GGA) was used in these calculations. The Vanderbilt ultrasoft pseudopotential [62] was applied. A 2 × 2 × 1 anatase supercell (48 atoms) was generated and an initial geometry optimization was carried out to confirm the viability of the experiment using methods previously used. It is well documented that the experimentally held crystallographic lattice parameters are a = 3.7845 and c = 9.5143. Therefore, it is important that computational relaxation reflects these values in simulation. Additionally, reproduction of the experimentally held band gap of 3.20 eV is of additional importance. Computationally reflecting these results has been proven successful by a variety of research groups. Table 1 reflects the findings of some of these groups and reports the lattice parameters and respective band gaps simulated.

Table 1: Previous findings for anatase titania

Authorship	***a = b***	***c***	***E_g***	***Ref #***
Li et al.	3.782	9.564	3.18	[49]
Long et al.	3.893	9.529	3.14	[51]
Yang et al.	3.776	9.485	3.58	[63]
Yu et al.	3.785	9.514	2.46*	[64]
Lichao et al.	3.818	9.480	3.08	[65]

Relaxation convergence criteria can be found in Table 2. It is well known that 48 atoms are more than sufficient for band structure simulations. However, convergence calculations were conducted to validate these system parameters for accuracy. Relaxation calculations for doped systems were only carried out for a 48 atom system as band structure simulations were the ultimate goal of this research.

Table 2: Convergence criteria for relaxation

Convergence Criteria	***Value***
Convergence Energy Tolerance	1×10^{-6} eV/atm
k-point	5×5×4
Max Force	.01 eV/ Å
Max Stress	.01 GPa
Max Displacement	.01 Å

Thermal stabilities of the doped systems were neglected as previous studies have shown negligible substitutional energy differences between doped systems and pure titania [49]. The total enthalpy of the doped systems can be found in Appendix A.

4.2 Band Structure Initialization

Band Structure calculations directly followed relaxation. Criteria remained the same for convergence with the exception of an inclusion of a U-correction for localized electrons. Six different initial nitrogen-transition metal co-doped systems were calculated to systematically confirm and compare their respective effect on the crystal titania system. Doped systems were constructed via atomic substitution. Transition metals and nitrogen were substituted into the crystal through replacement of titanium and oxygen, respectively. It is predicted that the presence of such nitrogen doping increases the VBM and the transition metal lowers the CBM as previous studies mentioned have shown. However, novel systems are also included which do not conform to the passivation methodology outlined by Gai et al. [56].

These non-passivated systems are included so as to determine the potential of titania as an extrinsic semiconductor for use within traditional solar cell technology. The unmatched electron is predicted to introduce localized states within the band gap and increase potential recombination sites. This study also aims to compare the effect of passivation on valence band and conduction band shifts within the crystal systems.

Energy calculation pathing within CASTEP was self-determined and confirmed to be consistent between doped systems. Figure 6 and 7 show the calculated pathing used within this thesis.

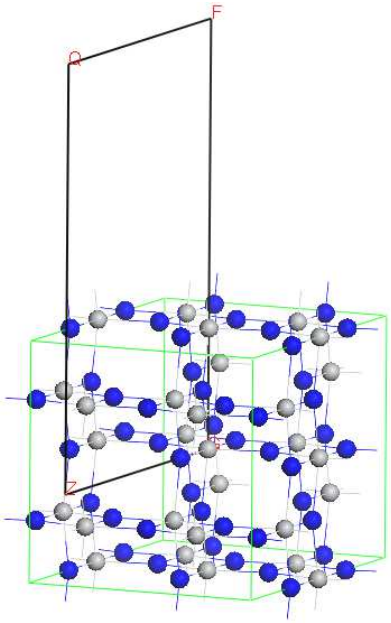

Figure 6: Un-doped anatase system pathing

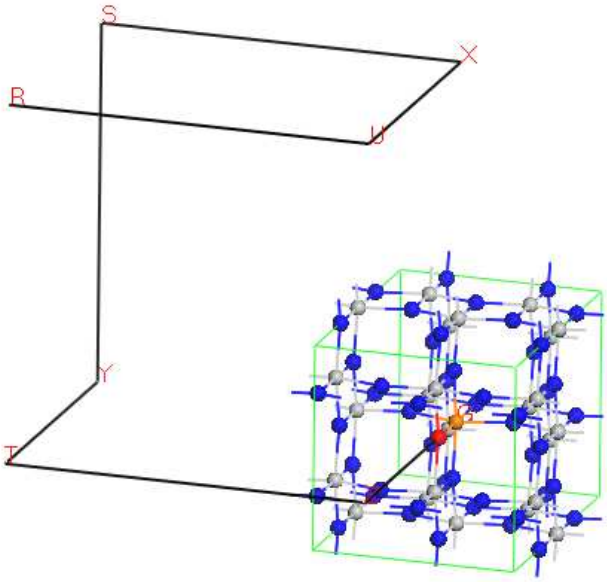

Figure 7: Doped anatase system pathing

4.3 Validation of Configuration

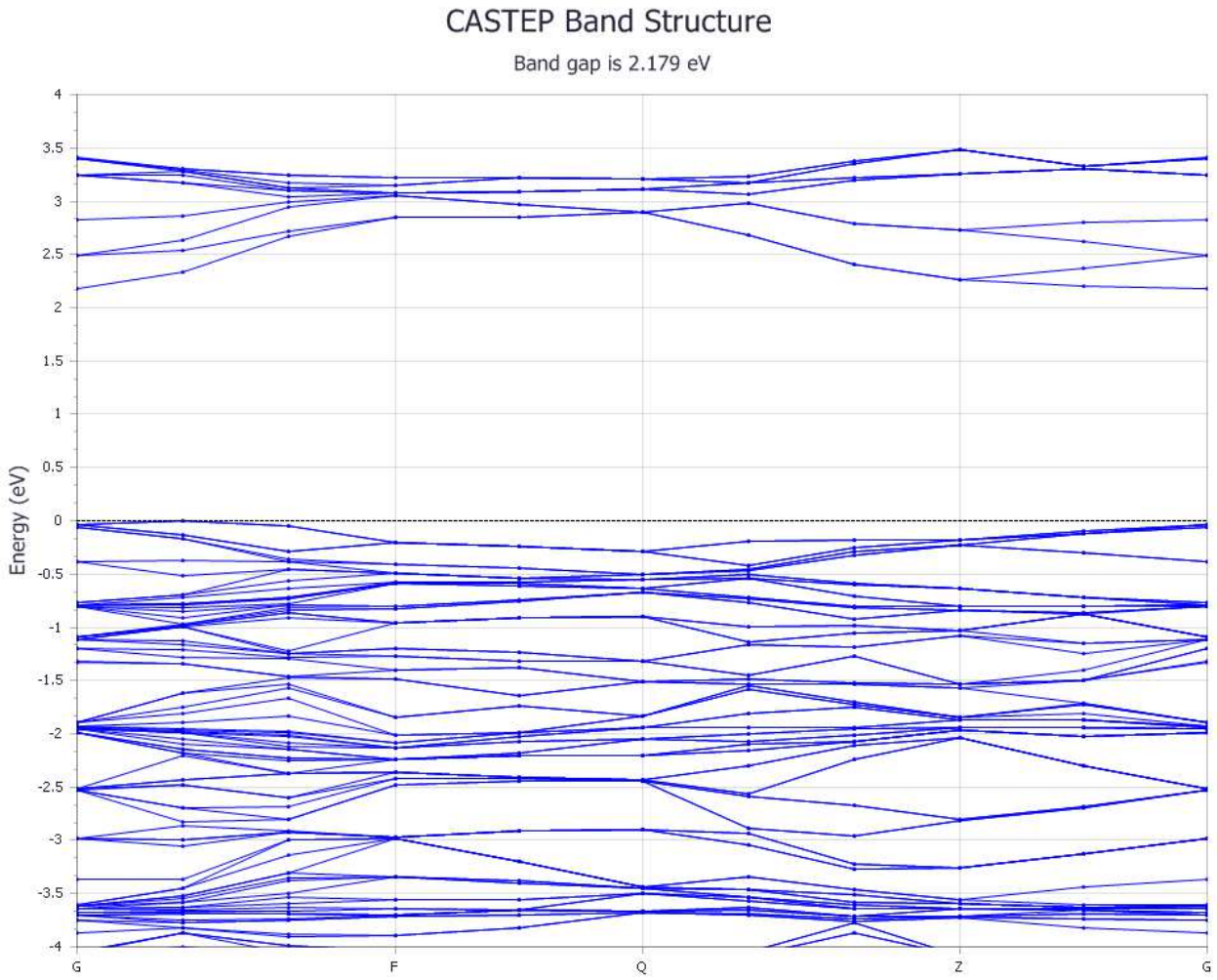

Figure 8: 48 atom un-doped anatase band structure plot

A system size convergence study was conducted for various atomic populations and it was confirmed that the crystal system's structure was well converged as the band gap and lattice parameters changed very little. Table 3, shown below, outlines the lattices parameters and band gap energy calculated from various system sizes. It becomes apparent that at 48 atoms the electronic energetic behavior of the crystal system is well converged.

The result achieved from GGA calculations without the Hubbard U-correction is in agreement with similar studies previously conducted [12] [66].

Table 3: system size convergence

System Size (atm)	***a (Å)***	***b (Å)***	***c (Å)***	***E_g (eV)***
6	3.7891728	3.7891728	9.7839948	2.160
12	3.7932575	3.7932575	9.7638949	2.160
24	3.79317585	3.7932119	9.7626368	2.183
48	3.79360535	3.79360525	9.7614638	2.179

4.4 GGA & GGA+U

It is extensively documented that the results of ab-initio band structure calculations drastically underestimate the band gap energy, specifically for those systems containing transition metals [67]. It has been shown that this consistent thematic undervaluation of transition metal band gaps is a result of over-binding on the part of the oxygen molecule within the transition metal oxide [68]. Localized electronic orbitals present within oxidation reaction result in consistent error in binding energy. This consequently results in an energy state less negative value than what is experimentally shown.

To correct for this binding energy error in transition metal oxides, the GGA+U method is introduced in electrical property simulations. This U-correction rectifies the difference in binding energies which are not cancelled out within the GGA formulism. The U-correction itself is an intra-atomic electron-electron term which more accurately formulates quantitative descriptions of the localized 3d orbitals of the titania crystal.

It is worth noting that there remains a sizeable difference in the lattice parameters when relaxation simulations are carried out with the additional U correction. Other research groups like Long et al. have come to the same conclusion that geometry optimization better reflects held

bond lengths and the GGA+U method is better suited solely for band-structure calculations [51]. Simulations were carried out to compare the two methods to confirm this assertion. It was confirmed that GGA exists as a better relaxation method.

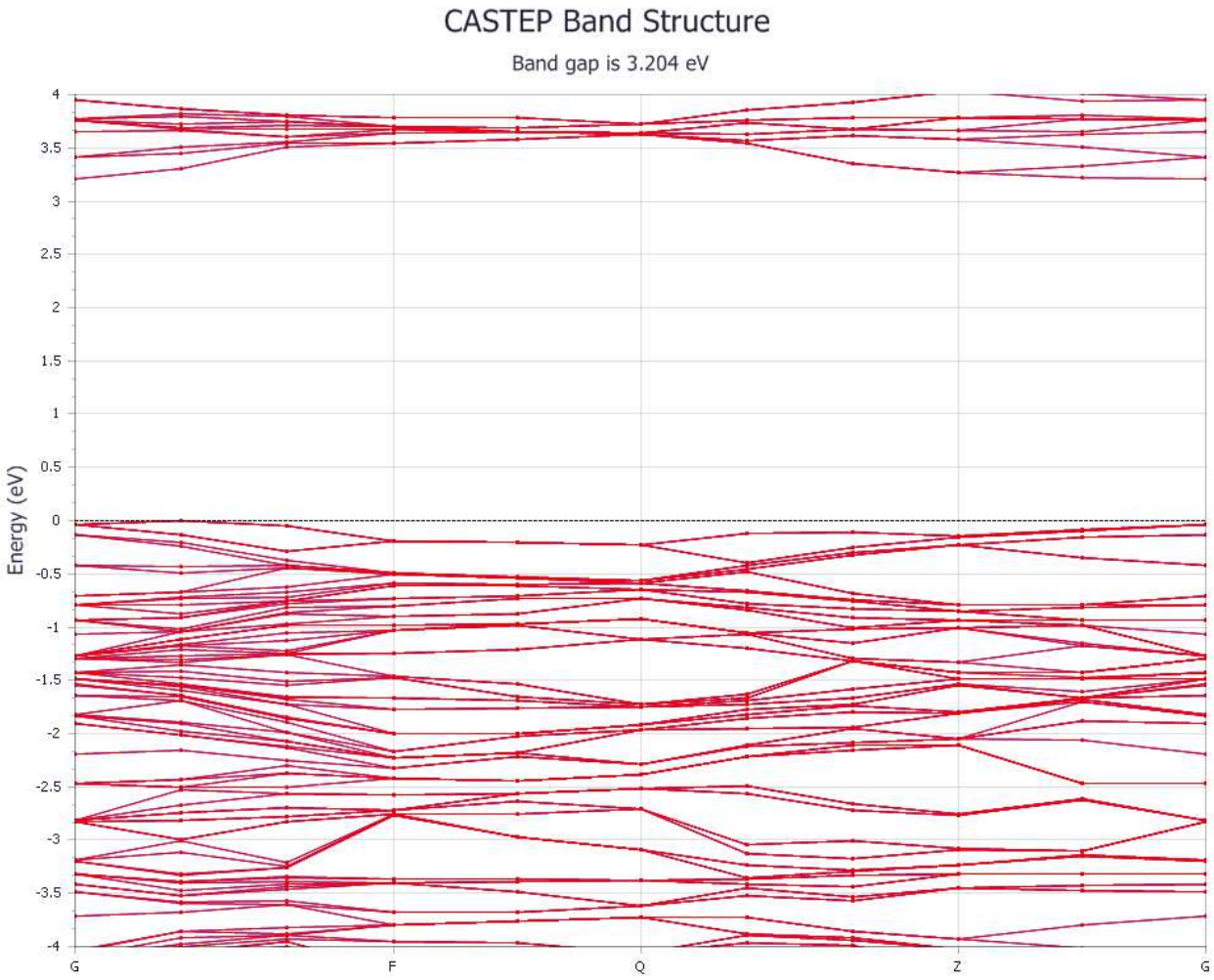

Figure 9: 48 atom anatase band structure plot with 8eV Hubbard correction

Additionally, GGA calculations were conducted on systems to confirm their inability to accurately formulate accurate energy and band structure calculations. It was confirmed that the GGA+U energy calculative method was several times more accurate than GGA alone.

Selection of U values is based on experimental findings from band gap studies of TiO_2. As it stands currently, 3.20 eV is the experimentally held band gap value for anatase titania. Consequently, electronic structural calculations must accurately reflect these values. It was found through successive calculations that a moderate correction of 8 eV best modeled the electronic structure of anatase titania. With an 8eV correction, a band gap of 3.204 eV was achieved. This experimentally determined value is in excellent agreement with experimentally verified systems.

CHAPTER 5

RESULTS AND DISCUSSION

5.1 Passivated System Results

Figure 10, shown below, reports the band structure diagram for the vanadium nitrogen co-doped titania system. From the diagram, the presence of these co-doping elements produces a shift in the characteristic CBM. New localized states are created which serve to reduce the band gap. These shallow local states present within the crystal's forbidden band gap remain the sole source for band gap reduction of about 1.2 eV.

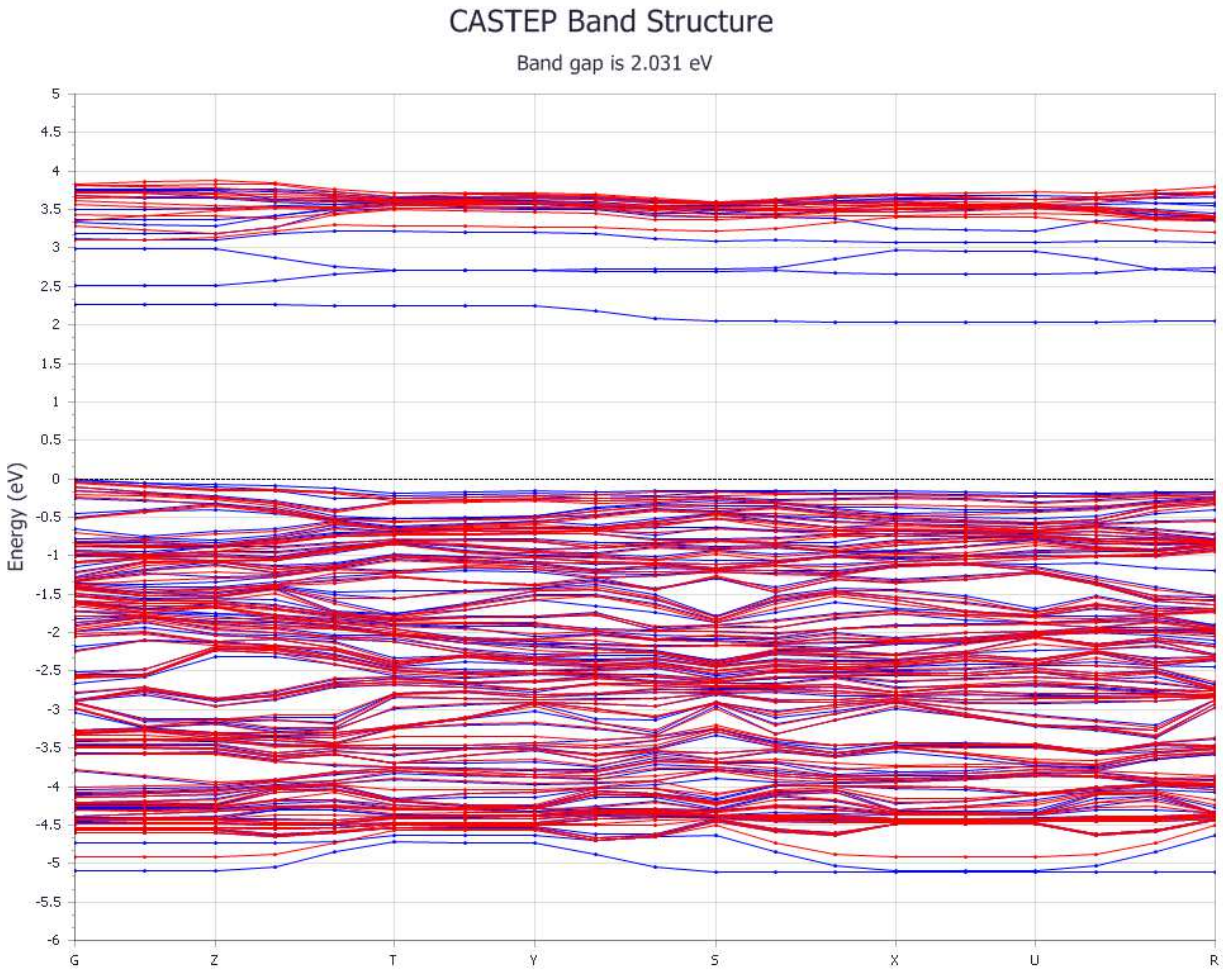

Figure 10: V-N co-doped anatase band-structure plot

The niobium nitrogen co-doped titania system exhibited a shift in both the CBM and the VBM. Figure 11 displays this distinguishing conduction band reduction of about .9 eV. As can be seen, the valence band is also reduced by .5 eV. With no apparent localized states present, niobium nitrogen co-doping directly modified the continuum of band structure.

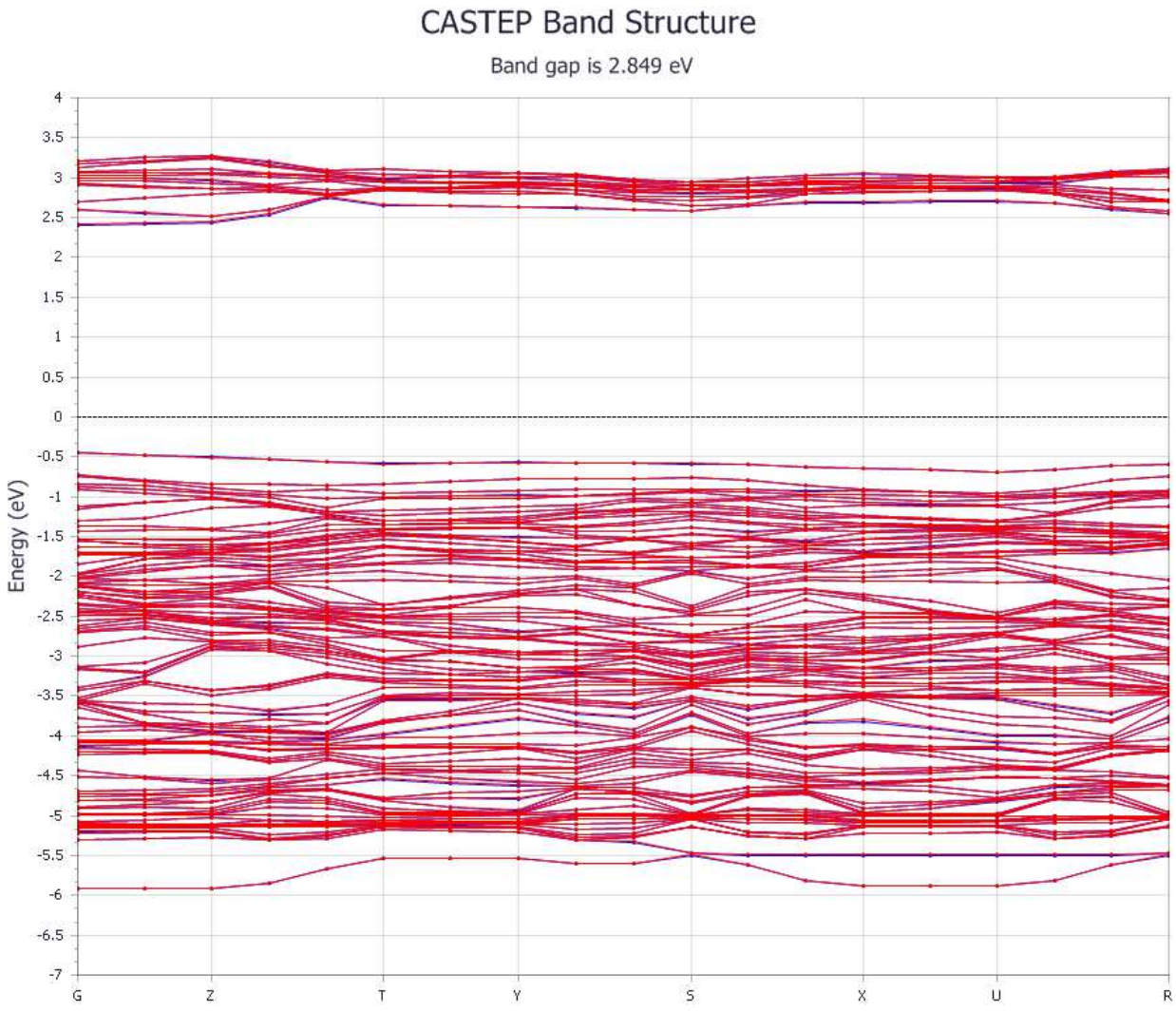

Figure 11: Nb-N co-doped anatase band-structure plot

Tantalum nitrogen co-doping presented band structure shifting in both valence and conduction bands. Additionally, shallow localized states become present in the forbidden band as possible trapping sites which can possibly reduce recombination. The conduction band continuum shifted by over .9 eV with the valence band continuum shifting again by about .5 eV.

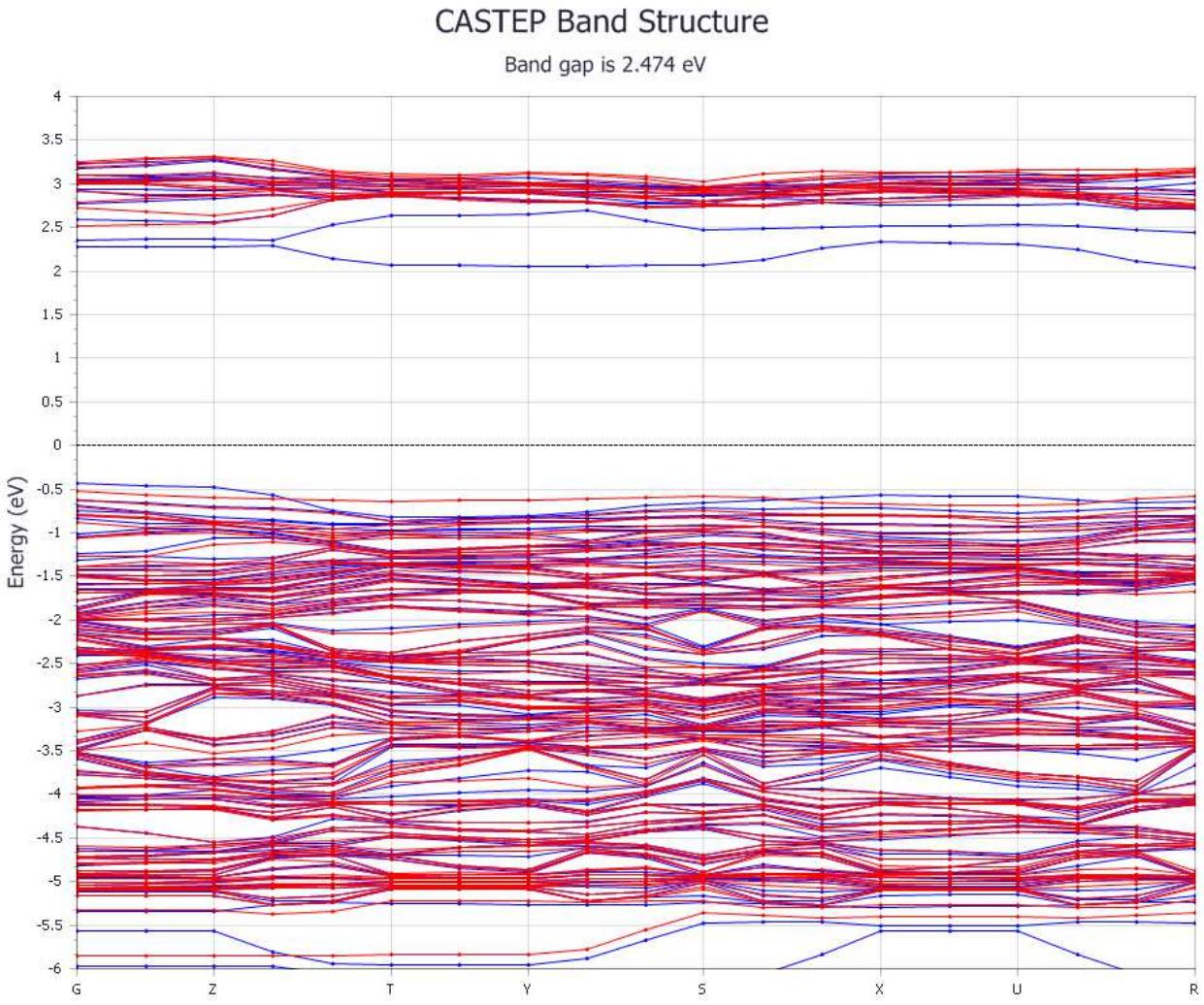

Figure 12: Ta-N co-doped anatase band-structure plot

5.2 Non-Passivated System Results

Non-passivated systems markedly changed the characteristic semiconducting behavior of the anatase crystal. Isolated impurity energy states became prevalent and persist deeper into the forbidden zone of the energy gap. A slight shift in the continuum of both valence and conduction bands can be seen in figure 13, which displays the band structure plot of chromium nitrogen co-doped titania. However, despite this shift, the localized states significantly affect the calculated band gap and aren't reflective of respective continuum energies.

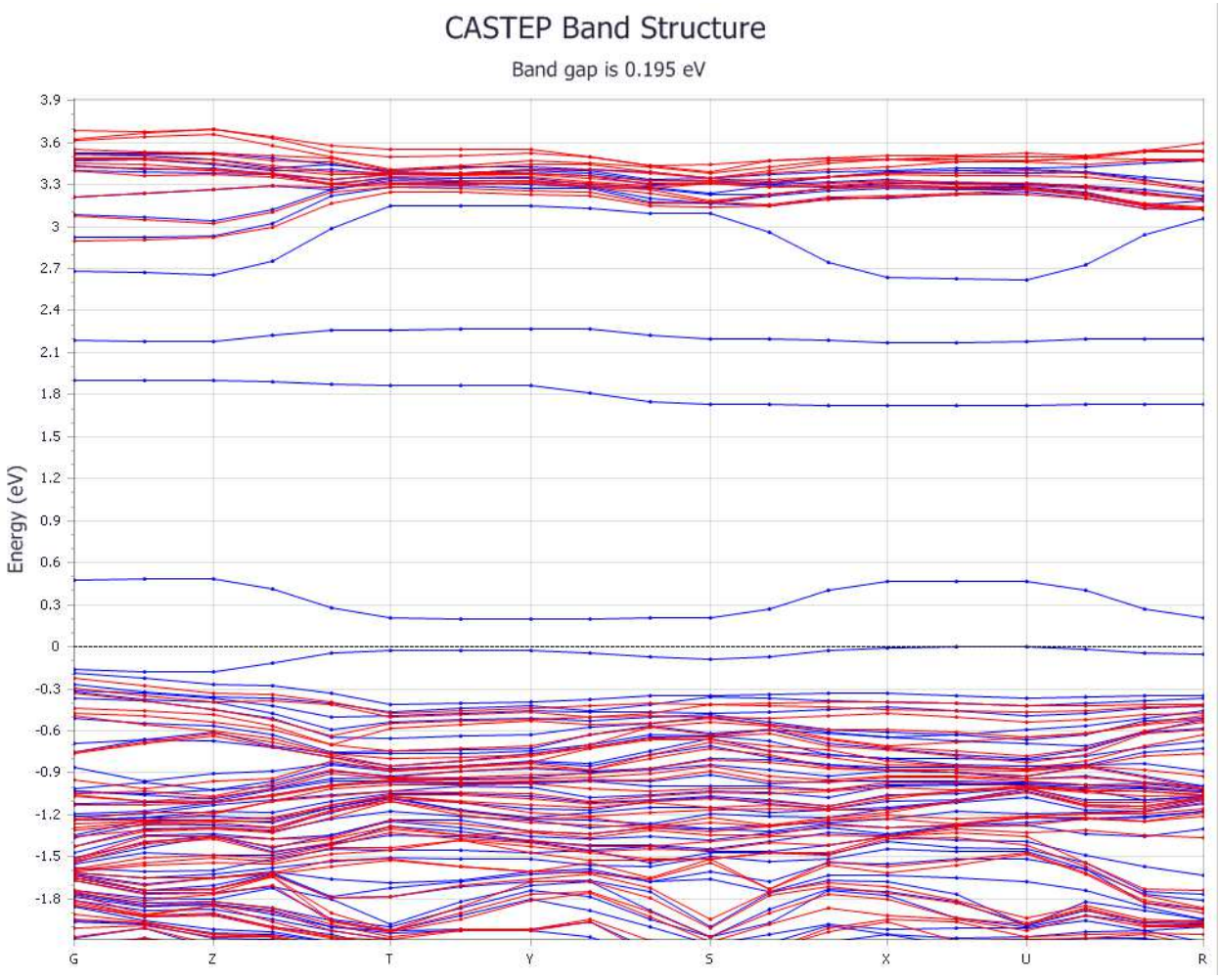

Figure 13:Cr-N co-doped anatase band-structure plot

The molybdenum nitrogen co-doped system distinctly changed in electronic structure from the previous system as localized systems become less frequent. However, there exists very little structural shifting of the valence and conduction bands. The resulting band gap of 1.272 eV as shown in figure 14 is representative of the impurity states still existent within the electronic structure.

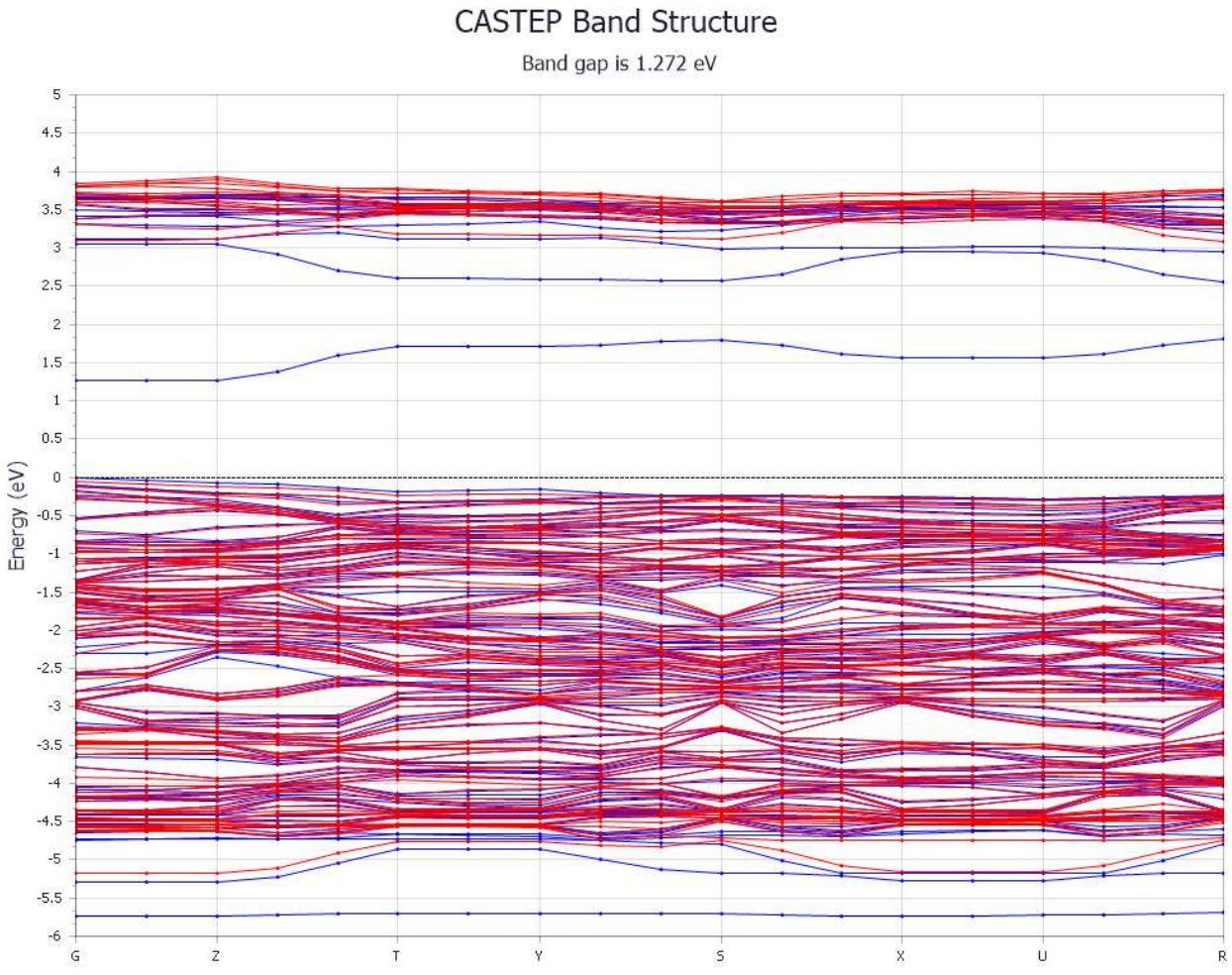

Figure 14: Mo-N co-doped anatase band-structure plot

Tungsten nitrogen co-doping presented an extremely large shift in the continuum of both valence and conduction bands. The conduction band was markedly reduced by roughly 1.6 eV. Concurrently, the valence band experienced a shift approaching 2.2 eV. Though reduced, the non-passivated system feature of impurity states prevalent within the forbidden band continues with this system. The resulting band gap of .742 is a result of these impurity states persistent within the electronic structure. The significant fermi level shift towards the conduction band alludes to probably n-type doping characteristics of tungsten nitrogen co-doping.

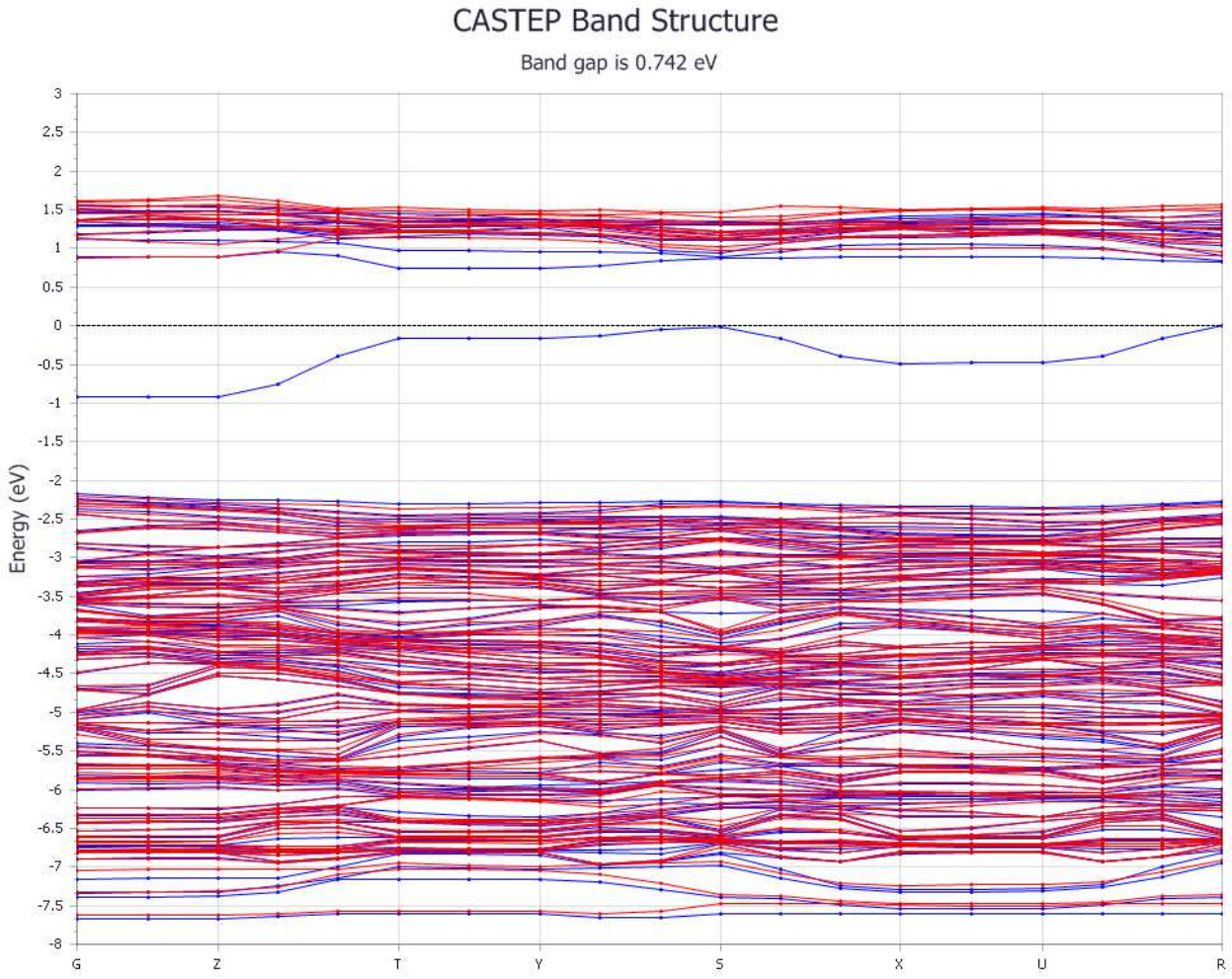

Figure 15: W-N co-doped anatase band-structure plot

Table 4: Dopant Effects

Dopant	**a (Å)**	**b (Å)**	**c (Å)**	**E_g (eV)**	**ΔE_g (eV)**
None	3.793606	3.793606	9.761464	3.204	0
V - N	3.806719	3.776441	9.729913	2.03	1.17
Nb - N	3.819588	3.790408	9.794828	2.85	.359
Ta - N	3.801952	3.839441	9.810859	2.47	.726
Cr - N	3.825896	3.774858	9.674787	.195	3.00
Mo - N	3.830475	3.791032	9.729327	1.27	1.93
W - N	3.8265465	3.799469	9.724496	.742	2.46

CHAPTER 6

CONCLUSION

6.1 Conclusion of Results

Chromium, molybdenum, tungsten, vanadium, niobium, and tantalum were individually co-doped with nitrogen into a 48 atom anatase titania crystal. Band structure analysis was used to compare those passivated and non-passivated systems. Fermi energy levels relative to the continuum of conduction and valence bands reveal characteristic shifts in semiconducting behavior in both systems.

Based on the results from the two disparate atomic substitutional types, passivated systems tend to produce fewer localized states and more effective narrowing of the electronic band gap. This shift in band structure suggests effective orbital hybridization and crystallinity in those passivated systems. The presence of shallow localized energy states in these systems suggest possible trapping sites which allude to possible reduced electronic recombination.

Passivated systems show this distinctive band gap narrowing through shifts in both conduction and valence bands. Additionally, this electronic structure shift is obtained with limited impact on crystal structure itself. However, as dopant levels were kept constant at 4.2%, it is uncertain to what extent these characteristics will continue with different doping percentages.

Non-passivated systems showed an erratic increase in localized states in the band structure which led to a misrepresentative decrease in band gap energy. These impurity states are thought to potentially significantly decrease photocatalytic performance in synthesized materials. These energy states are thought to provide recombination sites during excitation thereby mitigating band gap narrowing effects.

However, Tungsten-nitrogen co-doping presented an interesting feature within the simulations. A dramatic increase in the fermi level respective to band gap energy alludes to possible semiconducting behavior modification. Though unconfirmed, such behavior modification may prove to be of some use in future studies and materials development. Further studies are needed to confirm its potential viability.

These ab initio calculations conducted through the CASTEP package have ultimately shown to effectively describe the theoretical electronic structure of non-trivial atomic compositions.

6.2 Future Work

Future simulations with consideration to different passivated pair populations may prove to be useful in confirming the persistence of impurity states within the anatase band gap. Additionally, synthesis of these materials may further demonstrate the passivation methodology within the anatase electronic structure. Such synthesis further substantiates the reduction of band gap through the co-doping method. With additional time, further CASTEP analysis of the density of states and charge density differences may prove to be valuable.

BIBLIOGRAPHY

[1] A. Fujishima and K. Honda, "Electrochemical Photolysis of Water at a Semiconductor Electrode," *Nature,* vol. 238, no. 5358, pp. 37-38, 1972.

[2] R. Van Noort, "Titanium: The implant material of today," *Journal of Materials Science,* vol. 22, no. 11, p. 3801–3811, 1987.

[3] G. Pfaff and P. Reynders, "Angle-Dependent Optical Effects Deriving from Submicron Structures of Films and Pigments," *Chemical Reviews,* vol. 99, no. 7, p. 1963–1982, 1999.

[4] A. Mills and S. Le Hunte, "An overview of semiconductor photocatalysis," *Journal of Photochemistry and Photobiology A: Chemistry,* vol. 108, no. 1, p. 1–35, 1998.

[5] M. Zayat, P. Garcia-Parejo and D. Levy, "Preventing UV-light damage of light sensitive materials using a highly protective UV-absorbing coating," *Chemical Society Reviews,* vol. 36, no. 8, pp. 1270-1281, 2007.

[6] B. O'Regan and M. Grätzel, "Low-cost, high-efficiency solar cell based on dye-sensitized colloidal TiO2 films," vol. 353, no. 6346, pp. 737 - 740, 1991.

[7] X. Chen and S. S. Mao, "Titanium Dioxide Nanomaterials: Synthesis, Properties, Modifications, and Applications," *Chemical Reviews,* vol. 107, no. 7, p. 2891–2959, 2007.

[8] O. K. Varghese, D. Gong, M. Paulose, K. G. Ong and C. A. Grimes, "Hydrogen sensing using titania nanotubes," *Sensors and Actuators B: Chemical,* vol. 93, no. 1-3, p. 338–344, 2003.

[9] T. Luttrell, S. Halpegamage, J. Tao, A. Kramer, E. Sutter and M. Batzill, "Why is anatase a better photocatalyst than rutile? - Model studies on epitaxial TiO2 films," *Scientific Reports,* vol. 4, 2014.

[10] J. L. Giocondi, P. A. Salvador and G. S. Rohrer, "The origin of photochemical anisotropy in SrTiO3," *Topics in Catalysis,* vol. 44, no. 4, p. 529–533, 2007.

[11] G. Liu, L. Wang, H. G. Yang, H.-M. Cheng and G. Q. Lu, "Titania-based photocatalysts-crystal growth, doping and heterostructuring," *Journal of Materials Chemistry,* vol. 2, no. 5, pp. 831-843, 2010.

[12] F. Labat, P. Baranek, C. Domain, C. Minot and C. Adamo, "Density functional theory analysis of the structural and electronic properties of TiO2 rutile and anatase polytypes: Performances of different exchange-correlation functionals," *Journal of Chemical Physics,* vol. 126, no. 15, pp. 1-12, 2007.

[13] M. Xu, Y. Gao, E. M. Moreno, M. Kunst, M. Muhler, Y. Wang, H. Idriss and C. Wöll, "Photocatalytic Activity of Bulk TiO2 Anatase and Rutile Single Crystals Using Infrared Absorption Spectroscopy," *Physical Review Letters,* vol. 126, pp. 1-4, 2011.

[14] J. N. Wilson and H. Idriss, "Effect of surface reconstruction of TiO2(001) single crystal on the photoreaction of acetic acid," *Journal of Catalysis,* vol. 214, no. 1, pp. 46-52, 2003.

[15] Europa, "European Commission," DG Environment, 5 August 2016. [Online]. Available: http://ec.europa.eu/environment/chemicals/nanotech/. [Accessed 3 February 2017].

[16] O. K. Varghese, G. K. Mor, C. A. Grimes, M. Paulose and N. Mukherjee, "A titania nanotube-array room-temperature sensor for selective detection of hydrogen at low concentrations," *Journal of Nanoscience and Nanotechnology,* vol. 4, no. 7, pp. 733-737, 2004.

[17] O. Lisovski, A. Chesnokov, S. Piskunov, D. Bocharov, Y. F. Zhukovskii, M. Wessel and S. Eckhard, "Ab initio calculations of doped TiO2 anatase (101) nanotubes for photocatalytical water splitting applications," *Materials Science in Semiconductor Processing,* vol. 42, no. 1, pp. 138-141, 2015.

[18] J. Choi, H. Park and M. R. Hoffmann, "Effects of Single Metal-Ion Doping on the Visible-Light Photoreactivity of TiO2," *Journal of Physical Chemistry C,* vol. 114, no. 2, pp. 783-792, 2010.

[19] K. Nagaveni, M. S. Hegde and G. Madras, "Structure and Photocatalytic Activity of Ti1-xMxO2±δ(M = W, V, Ce, Zr, Fe, and Cu) Synthesized by Solution Combustion Method," *The Journal of Physical Chemistry B,* vol. 108, no. 52, pp. 20204-20212, 2004.

[20] A. Ghicov, J. M. Macak, H. Tsuchiya, J. Kunze, V. Haeublein, L. Frey and P. Schmuki, "Ion Implantation and Annealing for an," *Nano Letters,* vol. 6, no. 5, pp. 1080-1082, 2006.

[21] A. Mills, N. Elliott, I. P. Parkin, S. A. O'Neill and R. J. Clark, "Novel TiO2 CVD films for semiconductor photocatalysis," *Journal of Photochemistry and Photobiology A: Chemistry,* vol. 151, no. 1-3, pp. 171-179, 2002.

[22] B. T. Fichman, "U.S. Energy Information Administration," April 2016. [Online]. Available: http://www.eia.gov/energyexplained/?page=us_energy_home. [Accessed 16 February 2017].

[23] K. Nithyanandam and R. Pitchumani, "Analysis and design of dye-sensitized solar cell," *Solar Energy,* vol. 86, no. 1, pp. 351-368, 2012.

[24] L. Jiang, T. You and W.-Q. Deng, "Enhanced photovoltaic performance of a quantum dot-sensitized solar cell using a Nb-doped TiO2 electrode," *Nanotechnology,* vol. 24, no. 41, 2013.

[25] A. Ranjitha, N. Muthukumarasamy, M. Thambidurai, D. Velauthapillai, R. Balasundaraprabhu and S. Agilan, "CdS quantum dot sensitized nanocrystalline Gd-doped TiO2 thin films for photoelectrochemical solar cells," *Journal of Materials Science: Materials in Electronics,* vol. 24, no. 8, pp. 3014-3020, 2013.

[26] M. Dürr, S. Rosselli, A. Yasuda and G. Nelles, "Band-Gap Engineering of Metal Oxides for Dye-Sensitized Solar Cells," *Journal of Physical Chemistry B,* vol. 110, no. 43, pp. 21899-21902, 2009.

[27] B. Kılıç, N. Gedik, S. P. Mucur, A. S. Hergul and E. Gür, "Band gap engineering and modifying surface of TiO2 nanostructures by Fe2O3 for enhanced-performance of dye sensitized solar cell," *Materials Science in Semiconductor Processing,* vol. 31, no. 1, p. 363–371, 2015.

[28] D. Dvoranová, V. Brezová, M. Mazúr and M. A. Malati, "Investigations of metal-doped titanium dioxide photocatalysts," *Applied Catalysis B: Environmental,* vol. 37, no. 2, pp. 91-105, 2002.

[29] J. H. Park, S. Kim and A. . J. Bard, "Novel Carbon-Doped TiO2 Nanotube Arrays with High Aspect Ratios for Efficient Solar Water Splitting," *Nano Letters,* vol. 6, no. 1, pp. 24-28, 2005.

[30] Y. Cong, B. Tian and J. Zhang, "Improving the thermal stability and photocatalytic activity of nanosized titanium dioxide via La3+ and N co-doping," *Applied Catalysis B: Environmental,* vol. 101, no. 3-4, pp. 376-381, 2010.

[31] J. Zhang, X. Liu, S. Gao, Q. Liu, B. Huang and Y. Dai, "Preparation and Characterization of (I2)n Sensitized Nanoporous TiO2 with Enhanced Photocatalytic Activity under Visible-Light Irradiation," *International Journal of Photoenergy,* vol. 2012, no. 1, pp. 1-8, 2012.

[32] Y. Shao, L. F. Molnar and Y. Jung, "Advances in methods and algorithms in a modern quantum chemistry program package," *Physical Chemistry Chemical Physics,* vol. 8, no. 27, pp. 3172-3191, 2006.

[33] K. M. Glassford and J. R. Chelikowsky, "Structural and electronic properties of titanium dioxide," *Physical Review B,* vol. 46, no. 3, pp. 1284-1298, 1992.

[34] H. Kobayashi and M. Yamaguchi, "Ab initio MO study of adsorption of CO molecule on TiO2 surfaces," *Surface Science,* vol. 214, no. 3, pp. 466-476, 1989.

[35] D. C. Allan and M. P. Teter, "Local Density Approximation Total Energy Calculations for Silica and Titania Structure and Defects," *Journal of the American Ceramic Society,* vol. 73, no. 11, p. 3247–3250, 1990.

[36] M. Grätzel and F. P. Rotzinger, "The influence of the crystal lattice structure on the conduction band energy of oxides of titanium(IV)," *Chemical Physics Letters,* vol. 118, no. 5, pp. 474-477, 1985.

[37] M. Casarin, C. Maccato and A. Vittadini, "Density functional studies of molecular chemisorption on TiO2 (110)," *Applied Surface Science,* vol. 142, no. 1-4, pp. 196-199, 1999.

[38] W. Choi, A. Termin and M. R. Hoffmann, "The role of metal ion dopants in quantum-sized TiO2: Correlation between photoreactivity and charge carrier recombination dynamics," *Journal of Physical Chemistry,* vol. 98, no. 51, pp. 13669-13679, 1994.

[39] M. Anpo, Y. Ichihashi, M. Takeuchi and H. Yamashita, "Design of unique titanium oxide photocatalysts by an advanced metal ion-implantation method and photocatalytic reactions under visible light irradiation," *Research on Chemical Intermediates,* vol. 24, no. 2, pp. 143-149, 1998.

[40] R. Asahi, T. Morikawa, T. Ohwaki, K. Aoki and Y. Taga, "Visible-Light Photocatalysis in Nitrogen-Doped Titanium Oxides," *Science,* vol. 293, no. 5528, pp. 269-271, 2001.

[41] H. Irie, Y. Watanabe and K. Hashimoto, "Nitrogen-concentration dependence on photocatalytic activity of TiO2-xNx powders," *Journal of Physical Chemistry B,* vol. 107, no. 23, pp. 5483-5486, 2003.

[42] T. Ihara, M. Miyoshi, Y. Iriyama, O. Matsumoto and S. Sugihara, "Visible-light-active titanium oxide photocatalyst realized by an oxygen-deficient structure and by nitrogen doping," *Applied Catalysis B,* vol. 42, no. 4, pp. 403-409, 2003.

[43] C. Di Valentin, E. Finazzi, P. Gianfranco, A. Selloni, L. Stefano, M. C. Paganini and E. Giamello, "N-doped TiO2: Theory and experiment," *Chemical Physics,* vol. 339, no. 1-3, pp. 44-56, 2007.

[44] C. A. Harrison, Solid State Theory, New York: General Publishing Company, 1979.

[45] C. J. Ballhausen, Introduction to ligand field theory, Copenhagen: McGraw-Hill, 1962.

[46] U. Physics, "University of Tennessee Knoxville," 2008. [Online]. Available: www.phys.utk.edu/courses/Spring%202008/Physics%20555/Physics555Ch%209a.pdf. [Accessed 21 2 2017].

[47] W. Shockley, "The theory of p-n junctions in semiconductors and p-n junction transistors," *The Bell System Technical Journal,* vol. 28, no. 3, pp. 435-489, 1949.

[48] S. M. Sze and K. K. Ng, Physics of semiconductor devices, Hoboken: Wiley-Interscience, 2007.

[49] C. Li, Y. F. Zhao, Y. Y. Gong, T. Wang and C. Q. Sun, "Band gap engineering of early transition-metal-doped anatase TiO2: first principles calculations," *Physical Chemistry Chemical Physics,* vol. 16, no. 39, pp. 21446-21451, 2014.

[50] L. Mi, P. Xu, H. Shen and P.-N. Wang, "First-principles calculation of N:H codoping effect on energy gap narrowing of TiO2," *Applied Physics Letters,* vol. 90, no. 17, pp. 171909-171912, 2007.

[51] R. Long and N. J. English, "Band gap engineering of (N, Ta)-codoped TiO2: A first-principles calculation," *Chemical Physics Letters,* vol. 478, no. 4-6, p. 175–179, 2009.

[52] R. Long and N. J. English, "First principles calculation of nitrogen-tungsten codoping effects on the band structure of anatase-titania," *Applied Physics Letters,* vol. 94, no. 13, pp. 132102-132105, 2009.

[53] R. Long and N. J. English, "Electronic structure of cation-codoped TiO 2 for visible-light photocatalyst applications from hybrid density functional theory calculations," *Applied Physics Letters,* vol. 98, no. 14, pp. 142103-142103-3, 2011.

[54] D. J. Thouless, "Anderson's theory of localized states," *Journal of Physics C,* vol. 3, no. 7, pp. 1559-1566, 1970.

[55] C. Di Valentin, G. Pacchioni and A. Selloni, "Theory of carbon doping of titanium dioxide," *Chemistry of Materials,* vol. 17, no. 26, pp. 6656-6665, 2005.

[56] Y. Gai, J. Li, S.-S. Li, J.-B. Xia and S.-H. Wei, "Design of narrow-gap TiO2: A passivated codoping approach for enhanced photoelectrochemical activity," *Physical Review Letters,* vol. 102, no. 3, pp. 036402-1-036402-4, 2009.

[57] M. D. Segall, P. J. D. Lindan, M. J. Probert, C. J. Pickard, P. J. Hasnip, S. J. Clark and M. C. Payne, "First-principles simulation: ideas, illustrations and the CASTEP code," *Journal of Physics: Condensed Matter,* vol. 14, no. 11, pp. 2717-2744, 2002.

[58] P. Hohenberg and W. Kohn, "Inhomogeneous Electron Gas," *Physical Review,* vol. 136, no. 3B, pp. B864 - B871, 1964.

[59] M. T. Lusk and A. E. Mattsson, "High-performance computing for materials design to advance energy science," *MRS Bulletin,* vol. 36, no. 3, pp. 169-174, 2011.

[60] M. C. Payne, M. P. Teter, D. C. Allan, T. A. Arias and J. D. Joannopoulos, "Iterative minimization techniques for ab initio total-energy calculations: molecular dynamics and conjugate gradients," *Reviews of Modern Physics,* vol. 64, no. 4, pp. 1045-1097, 1992.

[61] J. P. Perdew, K. Burke and M. Ernzerhof, "Generalized Gradient Approximation Made Simple," *Physical Review Letters,* vol. 77, no. 18, pp. 3865-3868, 1996.

[62] D. Vanderbilt, "Soft self-consistent pseudopotentials in a generalized eigenvalue formalism," *Physical Review B,* vol. 41, no. 11, pp. 7892-7895, 1990.

[63] K. Yang, Y. Dai and B. Huang, "Origin of the photoactivity in boron-doped anatase and rutile TiO2 calculated from first principles," *Physical Review B,* vol. 76, no. 19, 2007.

[64] J. Yu, Q. Xiang and M. Zhou, "Preparation, characterization and visible-light-driven photocatalytic activity of Fe-doped titania nanorods and first-principles study for electronic structures," *Applied Catalysis B,* vol. 90, no. 3, pp. 595-602, 2009.

[65] J. Lichao, W. Congcong, H. Song, Y. Nian, L. Yuanyuan, L. Zongbao, B. Chi, J. Pu and J. Li, "Theoretical study on the electronic and optical properties of (N, Fe)-codoped anatase TiO2 photocatalyst," *Journal of Alloys and Compounds,* vol. 509, no. 20, p. 6067–6071, 2011.

[66] B. Prasai, B. Cai, M. K. Underwood, J. P. Lewis and D. A. Drabold, "Properties of amorphous and crystalline titanium oxide from first principles," *Journal of Material Science,* vol. 47, no. 21, pp. 7515-7521, 2012.

[67] S. P. Ong, "Materials Project," 13 September 2016. [Online]. Available: https://www.materialsproject.org/wiki/index.php/GGA%2BU_calculations#cite_note-1. [Accessed 14 March 2017].

[68] L. Wang, T. Maxisch and G. Ceder, "Oxidation energies of transition metal oxides within the GGA+U framework," *Physical Review B - Condensed Matter and Materials Physics,* vol. 73, no. 19, pp. 195107-1-195107-6, 2006.

[69] A. f. S. Energy, "NREL: Photovoltaic Research," 2017. [Online]. Available: https://www.nrel.gov/pv/assets/images/efficiency-chart.png. [Accessed 27 2 2017].

[70] M. Seery, "The Photochemistry Portal," 17 August 2009. [Online]. Available: https://photochemistry.wordpress.com/2009/08/17/dye-sensitised-solar-cells-dssc/. [Accessed 27 February 2017].

[71] G. Sun, "INTECH," 1 April 2010. [Online]. Available: http://www.intechopen.com/books/advances-in-lasers-and-electro-optics/the-intersubband-approach-to-si-based-lasers. [Accessed 28 February 2017].

[72] A. Rockett, The Materials Science of Semiconductors, New York: Springer Science, 2008.

[73] W. Setyawan and S. Curtarolo, "High-throughput electronic band structure calculations: Challenges and tools," *Computational Materials Science,* vol. 49, no. 2, pp. 299-312, 2010.

VITA

Cameron Robert Thurston

223 Carrier Hall, University of Mississippi, Oxford MS 38655

207-239-2818 (Cell) cameronthurston@hotmail.com

Education

B.S. Physics May 2015, Rhodes College, Memphis, TN

M.S. Mechanical Engineering May 2017, University of Mississippi, Oxford, MS

Experience

Teaching Assistant, University of Mississippi, Oxford MS, Aug. 2015 – Present

Research Assistant, University of Mississippi, Oxford MS, Aug. 2015 – Present

NCPA Intern, University of Mississippi, Oxford MS, Jun. 2013 – Aug. 2013

Research Assistant, Rhodes College, Memphis TN, Jun. 2011 – Aug. 2012

Publications (in refereed journals)

"Backscatter difference techniques for bone assessment using an ultrasonic imaging system", B.K. Hoffmeister, M.R. Smathers, C.J. Miller, J.A. McPherson, C.R. Thurston, P.L. Spinolo, S. Lee, J. Acoust. Soc. Am. 137, 2287 (2015)

"A technique for measuring bone density using an ultrasonic imaging system", C.J. Miller, M.R. Smathers, C.R. Thurston, B.K. Hoffmeister, J. Acoust. Soc. Am. 134, 4120 (2013)